Hypoxia-inducible factor 1-dependent expression of adenosine receptor 2B promotes breast cancer stem cell enrichment

Jie Lan[a,b], Haiquan Lu[b,c], Debangshu Samanta[b,c], Shaima Salman[b,c], You Lu[a], and Gregg L. Semenza[b,c,d,e,f,g,h,1]

[a]Department of Thoracic Oncology, Cancer Center and State Key Laboratory of Biotherapy, West China Hospital, Sichuan University, Chengdu 610041, China; [b]Institute for Cell Engineering, Johns Hopkins University School of Medicine, Baltimore, MD 21205; [c]McKusick–Nathans Institute of Genetic Medicine, Johns Hopkins University School of Medicine, Baltimore, MD 21205; [d]Department of Pediatrics, Johns Hopkins University School of Medicine, Baltimore, MD 21205; [e]Department of Medicine, Johns Hopkins University School of Medicine, Baltimore, MD 21205; [f]Department of Oncology, Johns Hopkins University School of Medicine, Baltimore, MD 21205; [g]Department of Radiation Oncology, Johns Hopkins University School of Medicine, Baltimore, MD 21205; and [h]Department of Biological Chemistry, Johns Hopkins University School of Medicine, Baltimore, MD 21205

Contributed by Gregg L. Semenza, August 17, 2018 (sent for review June 6, 2018; reviewed by Jonathan Sleeman and Cormac T. Taylor)

Breast cancer stem cells (BCSCs), which are characterized by a capacity for unlimited self-renewal and for generation of the bulk cancer cell population, play a critical role in cancer relapse and metastasis. Hypoxia is a common feature of the cancer microenvironment that stimulates the specification and maintenance of BCSCs. In this study, we found that hypoxia increased expression of adenosine receptor 2B (A2BR) in human breast cancer cells through the transcriptional activity of hypoxia-inducible factor 1. The binding of adenosine to A2BR promoted BCSC enrichment by activating protein kinase C-δ, which phosphorylated and activated the transcription factor STAT3, leading to increased expression of interleukin 6 and NANOG, two key mediators of the BCSC phenotype. Genetic or pharmacological inhibition of A2BR expression or activity decreased hypoxia- or adenosine-induced BCSC enrichment in vitro, and dramatically impaired tumor initiation and lung metastasis after implantation of MDA-MB-231 human breast cancer cells into the mammary fat pad of immunodeficient mice. These data provide evidence that targeting A2BR might be an effective strategy to eradicate BCSCs.

oxygen | caffeine | tumor-initiating cells | HIF-1 | ADORA2B

Breast cancer is a major public health problem that affects women all over the world. According to 2017 data, there were over 250,000 new breast cancer cases and more than 40,000 breast cancer-related deaths in the United States alone (1). Breast cancer cells with stem cell-like properties (BCSCs) are a minority population of tumor cells that (*i*) give rise to both daughter BCSCs (self-renewal) and bulk cancer cells (2, 3); (*ii*) are resistant to therapy; and (*iii*) are responsible for initiating and propagating recurrent and metastatic tumors (4–6).

Hypoxia is a hallmark of cancer that contributes to metastasis, treatment failure, and patient mortality (7–9). Intratumoral hypoxia also increases the number of BCSCs (7, 10). The transcriptional response of cancer cells to intratumoral hypoxia is principally mediated by hypoxia-inducible factors (HIFs), which are composed of an O_2-regulated HIF-α subunit (HIF-1α, HIF-2α, or HIF-3α) and a constitutively expressed HIF-1β subunit (7, 11, 12). Under hypoxic conditions, extracellular ATP is metabolized to ADP and AMP by CD39, and AMP is metabolized to adenosine by CD73 (13, 14). Adenosine is a ubiquitous nucleoside that regulates various physiological functions, with normal tissue levels of 10–200 nM, which can increase to 10–100 μM under hypoxic or ischemic conditions (15, 16). In tumors, high levels of adenosine modulate the functions of both tumor cells and tumor-infiltrating immune cells to promote cancer progression (14, 15).

Adenosine elicits biological responses by interacting with its four cognate transmembrane receptors (A1R, A2AR, A2BR, and A3R), which belong to the G-protein–coupled receptor superfamily (17). By binding to A1R or A3R, adenosine negatively regulates adenylyl cyclase, thereby reducing cAMP production (18), whereas by binding to A2AR or A2BR, adenosine increases cAMP production, leading to activation of protein kinase A (PKA) (19, 20) and phospholipase C (PLC) (21). A2BR expression was induced in a HIF-1α–dependent manner by exposure of cultured mouse intestinal epithelial cells to hypoxia (22). Hypoxia-induced expression of A2BR leads to increased signal transduction (23).

Critical roles for A2BR in stimulating tumor progression have been reported recently. In the Lewis lung carcinoma mouse model, A2BR activation promoted the expansion of myeloid-derived suppressor cells, which blocked T cell-mediated antitumor immunity (24). In prostate cancer cell lines, A2BR signaling increased cell proliferation and tumor growth (25, 26). A2BR signaling in breast cancer cells promoted filopodia formation, invasion, and metastasis (27–30). However, whether A2BR signaling affects the stem-like capacity of breast cancer cells is unknown. In the present work, we demonstrate that A2BR signaling is required for induction of the BCSC phenotype in response to hypoxia and delineate the signal transduction pathway that leads from A2BR to expression of the pluripotency factor NANOG.

Results

Hypoxia Induces A2BR Expression in Breast Cancer Cells. We previously found that hypoxia increases the production of adenosine

Significance

In order for a single breast cancer cell to form a recurrent tumor after therapy or a metastasis at a distant site such as the lung, it must have the properties of a breast cancer stem cell. In this paper, we show that adenosine receptor 2B (A2BR) plays a critical role in breast cancer stem cell specification. Adenosine receptor 2A (A2AR) signaling has been shown to play an important role in enabling cancer cells to evade antitumor immunity and A2AR-selective inhibitors are in clinical trials. Our results suggest that inhibiting A2BR may also provide therapeutic benefit to breast cancer patients.

Author contributions: G.L.S. designed research; J.L., H.L., D.S., and S.S. performed research; Y.L. contributed new reagents/analytic tools; J.L. and G.L.S. analyzed data; and J.L. and G.L.S. wrote the paper.

Reviewers: J.S., University of Heidelberg; and C.T.T., University College Dublin Conway Institute.

The authors declare no conflict of interest.

[1]To whom correspondence should be addressed. Email: gsemenza@jhmi.edu.

This article contains supporting information online at www.pnas.org/lookup/suppl/doi:10.1073/pnas.1809695115/-/DCSupplemental.

Published online September 21, 2018.

due to HIF-dependent activation of *CD73* gene expression in several triple-negative breast cancer (TNBC) cell lines, which lack expression of the estrogen receptor (ER), progesterone receptor (PR), and HER2 (31). Based on this finding, we hypothesized that adenosine receptor expression may also be induced by intratumoral hypoxia in human breast cancers. To test this hypothesis, we first analyzed whether the expression of mRNAs encoding adenosine receptors is correlated with the expression of a HIF metagene signature composed of 10 HIF target-gene mRNAs (ANGPTL4, LDHA, PGK1, CA9, CXCR3, L1CAM, BNIP3, PLOD1, P4HA1, and P4HA2) in 1,095 human breast cancer specimens from The Cancer Genome Atlas (TCGA) database using the Pearson correlation test. Among the four adenosine receptors, only A2BR mRNA expression was significantly correlated with expression of the HIF metagene signature (Fig. 1*A*). We next analyzed A2BR mRNA expression in different molecular subtypes of breast cancer (luminal A, luminal B, HER2-enriched, and basal-like), which are based on a 50-mRNA (PAM50) signature (32). Compared with each of the other molecular subtypes, A2BR mRNA levels were significantly increased in basal-like breast cancers (Fig. 1*B*), in which expression of HIF target genes is also increased relative to the other subtypes (33).

To investigate whether hypoxia increases A2BR expression in human breast cancer cells, the TNBC cell lines SUM149 and SUM159, and the ER^+PR^+ cell lines MCF-7 and BT474, were exposed to 1% or 20% O_2 for 24 h. Reverse transcription and quantitative real-time PCR (RT-qPCR) analysis of total RNA isolated from the cells revealed that exposure to 1% O_2 increased A2BR mRNA expression in all four cell lines (Fig. 1*C*), whereas mRNA encoding the other three adenosine receptors showed no consistent increase among the four cell lines (*SI Appendix*, Fig. S1). A2BR protein expression was increased in all four breast cancer cell lines after 48-h exposure to 1% O_2 (Fig. 1*D*). Next, flow cytometry was performed to detect cell surface expression of A2BR. After exposure to 1% O_2 for 48 h, the

A

Correlation between HIF signature and adenosine receptor mRNA

	A1R	A2AR	A2BR	A3R
vs. HIF-1 (R)	0.012	0.009	0.361	-0.005
vs. HIF-1 (p)	0.776	0.833	<0.001	0.914

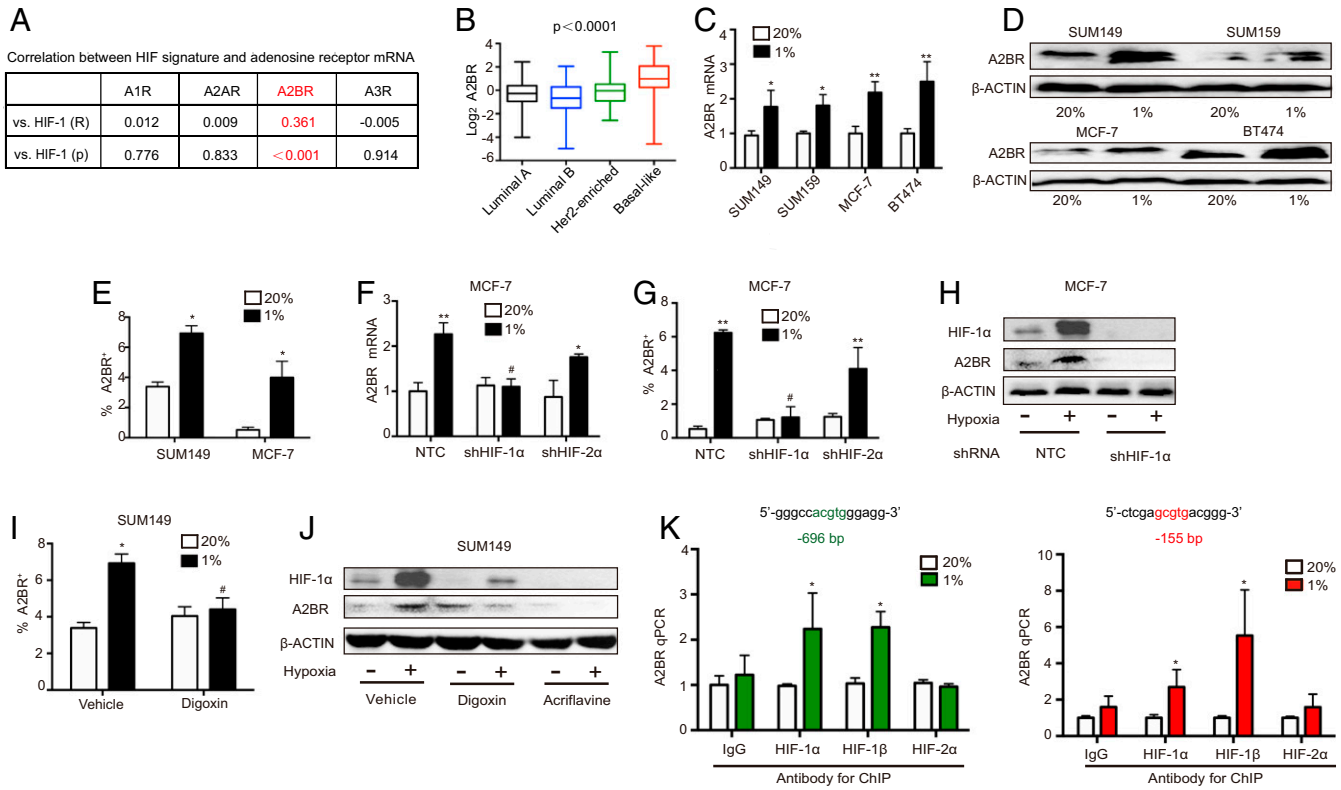

Fig. 1. Hypoxia induces A2BR expression in a HIF-1–dependent manner. (*A*) The expression level of mRNAs encoding the four adenosine receptors (A1R, A2AR, A2BR, A3R) in each of 1,095 human breast cancers from TCGA database were compared with a 10-mRNA HIF target-gene signature. For each comparison, the Pearson correlation coefficient (*R*) and statistical significance (*P*) are shown. (*B*) The relative $\log_2$ expression of A2BR mRNA from 1,095 human breast cancer specimens that were stratified according to molecular subtype is shown. Statistical analysis was performed by one-way ANOVA. Post hoc testing demonstrated significantly increased A2BR expression in basal-like tumors compared with each of the other subtypes. (*C* and *D*) Four human breast cancer cell lines were exposed to 20% or 1% O_2 for 24 h (*C*) or 48 h (*D*), and the expression of A2BR mRNA (*C*) or protein (*D*) was analyzed by RT-qPCR (*C*) and immunoblot (*D*) assays. For each cell line, the expression of A2BR mRNA was quantified relative to 18S rRNA and then normalized to the result obtained from cells at 20% O_2 (mean ± SD; $n = 3$). $^*P < 0.05$, $^{**}P < 0.01$ versus 20% O_2 (one-way ANOVA). (*E*) Cells were exposed to 20% or 1% O_2 for 48 h, and the percentage of cells expressing A2BR was determined by flow cytometry (mean ± SD; $n = 3$). $^*P < 0.05$ versus 20% O_2 (one-way ANOVA). (*F* and *G*) MCF-7 subclones, which stably expressed a nontargeting control shRNA (NTC), or shRNA targeting HIF-1α (shHIF-1α) or HIF-2α (shHIF-2α), were exposed to 20% or 1% O_2 for 24 h, followed by analysis of A2BR mRNA levels by RT-qPCR (*F*), or for 48 h, followed by analysis of $A2BR^+$ cells by flow cytometry (*G*) (mean ± SD; $n = 3$). $^*P < 0.05$, $^{**}P < 0.01$ versus NTC at 20% O_2; $^{\#}P < 0.05$ versus NTC at 1% O_2 (two-way ANOVA). (*H*) A2BR and HIF-1α expression were determined by immunoblot assay in MCF-7 subclones exposed to 20% or 1% O_2 for 48 h. (*I*) SUM149 cells were exposed to 20% or 1% O_2, in the presence of vehicle or digoxin (100 nM) for 48 h, and the percentage of $A2BR^+$ cells was determined (mean ± SD; $n = 3$). $^*P < 0.05$ versus vehicle at 20% O_2; $^{\#}P < 0.05$ versus vehicle at 1% O_2 (two-way ANOVA). (*J*) A2BR expression was determined in SUM149 cells exposed to 20% or 1% O_2 for 48 h in the presence of vehicle, digoxin (100 nM), or acriflavine (1 μM). (*K*) MCF-7 cells were exposed to 20% or 1% O_2 for 16 h, and ChIP assays were performed using IgG or antibodies against HIF-1α, HIF-1β, or HIF-2α. Primers flanking candidate HIF binding sites at −696 bp (*Left*) and −155 bp (*Right*) relative to the transcription initiation site were used for qPCR, and results were normalized to chromatin immunoprecipitated with IgG from cells exposed to 20% O_2 (mean ± SD; $n = 3$). $^*P < 0.05$ vs. 20% O_2 (two-way ANOVA).

percentage of A2BR$^+$ cells increased twofold in SUM149 and 5.5-fold in MCF-7 cells (Fig. 1*E*) based on flow cytometry (*SI Appendix*, Fig. S2). Taken together, these data indicate that hypoxia induces increased A2BR mRNA and protein expression in human breast cancer cell lines.

Hypoxia-Induced A2BR Expression Is HIF-1α Dependent. Next, we analyzed whether HIF knockdown by stable expression of short hairpin RNA (shRNA) in MCF-7 cells (34) blocked A2BR induction in response to hypoxia. RT-qPCR (Fig. 1*F*) and flow cytometry (Fig. 1*G*) revealed that HIF-1α knockdown, but not HIF-2α knockdown, blocked the induction of A2BR mRNA (Fig. 1*F*) and cell surface protein (Fig. 1*G*) expression in cells exposed to 1% O_2. Immunoblot assays revealed hypoxic induction of A2BR and HIF-1α expression in MCF-7 cells that were stably transduced with lentiviral vector encoding a nontargeting control (NTC) shRNA, whereas hypoxic induction of these proteins was abrogated by expression of shRNA targeting HIF-1α (Fig. 1*H*).

To complement these RNA interference studies, we took a pharmacologic approach by treating cells with digoxin or acriflavine, which inhibit HIF-1 activity in hypoxic cells by distinct molecular mechanisms: Digoxin blocks HIF-1α protein accumulation (35), whereas acriflavine blocks the dimerization of HIF-1α with HIF-1β, which subsequently leads to degradation of HIF-1α (36). Treatment of SUM149 cells with either digoxin or acriflavine blocked hypoxia-induced A2BR expression as determined by flow cytometry (Fig. 1*I*) and immunoblot assays (Fig. 1*J*).

To determine whether HIF-1 directly binds to the *ADORA2B* gene encoding A2BR and activates its transcription in hypoxic MCF-7 cells, chromatin immunoprecipitation (ChIP) assays were performed to evaluate candidate HIF-1 binding sites that matched the consensus sequence 5′-(A/G)CGTG-3′ (37). Chromatin fragments containing either of two DNA sequences located in the 5′-flanking region of the *ADORA2B* gene at −696 bp (Fig. 1*K*, *Left*) and −155 bp (Fig. 1*K*, *Right*) relative to the transcription start site were immunoprecipitated with antibody against either HIF-1α or HIF-1β, but not HIF-2α, in a hypoxia-inducible manner. Taken together, the data presented in Fig. 1 demonstrate that A2BR expression is induced by exposure of ER$^+$ and ER$^-$ breast cancer cells to hypoxia in a HIF-1α–dependent manner. The significant correlation between HIF target gene expression and A2BR mRNA levels in human breast cancers suggests that HIF-1 also plays a critical role in regulating *ADORA2B* gene expression in vivo.

A2BR Mediates BCSC Enrichment. Hypoxia promotes the maintenance and specification of BCSCs and promotes tumor metastasis (7–10). To determine whether A2BR contributes to BCSC enrichment in response to hypoxia, we cultured SUM149 and MCF-7 cells on ultra-low attachment plates as mammospheres, which are enriched for BCSCs (38). A2BR mRNA expression was increased in mammospheres compared with monolayer cultures of SUM149 (Fig. 2*A*, *Upper*) or MCF-7 cells (Fig. 2*A*, *Lower*). Increased aldehyde dehydrogenase (ALDH) activity is another feature of BCSCs (39). We stained for ALDH activity and A2BR expression to determine whether they colocalize to the same cells. Flow cytometry demonstrated that the percentage of ALDH$^+$A2BR$^+$ cells was significantly increased by greater than fourfold after exposure of SUM149 or MCF-7 cells to 1% O_2 for 72 h (Fig. 2*B* and *SI Appendix*, Fig. S3).

To define the role of A2BR in hypoxia-induced BCSC enrichment, we generated A2BR knockdown subclones by stably transducing SUM149, MCF-7, or MDA-MB-231 cells with lentiviral vectors encoding one of five different shRNAs against A2BR, or a vector expressing NTC shRNA (*SI Appendix*, Fig. S4). The number of mammosphere-forming cells (Fig. 2*C*) was increased in response to hypoxia in NTC subclones but not in A2BR-knockdown subclones of SUM149 and MCF-7 cells (Fig. 2D). Consistently, the percentage of ALDH$^+$ cells induced by hypoxia was significantly decreased by A2BR knockdown in SUM149, MDA-MB-231, and MCF-7 cells (Fig. 2*E* and *SI Appendix*, Fig. S5).

To further confirm the function of A2BR in BCSC enrichment, MCF-7 cells were treated with an A2BR-specific antagonist, alloxazine, or a pan-adenosine receptor antagonist, caffeine, during exposure to 20% or 1% O_2. Compared with vehicle-treated cells, pharmacological inhibition of adenosine receptors by alloxazine or caffeine blocked the increase in ALDH$^+$ cells that was induced by hypoxia (Fig. 2*F*). Treatment of SUM149, MCF-7, and MDA-MB-231 cells with adenosine under non-hypoxic conditions increased the percentage of ALDH$^+$ BCSCs (Fig. 2*G*), and this increase was abrogated by A2BR knockdown in MCF-7 (Fig. 2*H*) and MDA-MB-231 (Fig. 2*I*) cells. Taken together, these data indicate that A2BR expression is required for hypoxia- or adenosine-induced BCSC enrichment.

A2BR Knockdown Impairs Tumor Formation and Decreases BCSCs in Vivo. To investigate the effect of A2BR knockdown on the tumorigenic capacity of breast cancer cells, which is a measure of the BCSC population, we injected a limiting number (1×10^3) of MDA-MB-231 NTC or either of two independent A2BR-knockdown subclones (sh1 or sh4) cells into the mammary fat pad (MFP) of female severe combined immunodeficiency (SCID) mice. Eleven weeks after injection, 100% of the mice (8 of 8) injected with NTC cells had developed palpable tumors, whereas only 12.5% (2 of 16) of mice injected with A2BR knockdown cells developed tumors (Fig. 3*A*).

As only BCSCs can give rise to a clinically relevant metastasis, we hypothesized that A2BR knockdown would impair lung metastasis. To test the hypothesis, we injected 2×10^6 MDA-MB-231 NTC or A2BR-knockdown cells into the MFP of SCID mice. As shown in Fig. 3*B*, when large numbers of cells were implanted, primary tumor growth curves were not significantly different between the NTC and A2BR knockdown subclones. When tumor volume reached 1,200 mm^3, tumor and lung tissues were collected. A2BR-knockdown primary tumors contained significantly decreased numbers of BCSCs as determined by mammosphere (Fig. 3*C*) and ALDH (Fig. 3*D*) assays. Hematoxylin and eosin staining of lung sections revealed that knockdown of A2BR completely blocked lung metastasis (Fig. 3 *E* and *F*). Taken together, the data presented in Fig. 3 indicate that A2BR is critical for tumor initiation and lung metastasis, both of which are mediated by BCSCs.

A2BR Mediates BCSC Enrichment Through PKCδ-Dependent STAT3 Activation. A2BR is a G-protein–coupled receptor, stimulation of which usually leads to cAMP-dependent activation of PKA (40, 41). To investigate the molecular mechanism through which A2BR promotes BCSC enrichment, we first treated MCF-7 cells with the PKA inhibitor H-89, which failed to block adenosine-induced enrichment of ALDH$^+$ cells (*SI Appendix*, Fig. S6*A*). We next treated cells with either of two general inhibitors of protein kinase C (PKC), Ro31-8220 and sotrastaurin, which blocked adenosine-induced ALDH activity in MCF-7 (Fig. 4 *A* and *B*) and MDA-MB-231 (*SI Appendix*, Fig. S6*B*) cells.

PKC family members can be divided into Ca^{2+}-dependent and Ca^{2+}-independent isoforms. Treatment of MCF-7 cells with Gö6976 to inhibit the catalytic activity of Ca^{2+}-dependent PKC isoforms (PKCα and PKCβ1) failed to block adenosine-mediated induction of ALDH$^+$ cells (Fig. 4*C*). In contrast, treatment with i-PKCδ, a peptide that selectively blocks the catalytic activity of the Ca^{2+}-independent isoform PKCδ, completely abrogated adenosine-induced ALDH activity in MCF-7 (Fig. 4*D*) and MDA-MB-231 (*SI Appendix*, Fig. S6*B*) cells. Immunoblot assays revealed that PKCδ was phosphorylated in response to adenosine

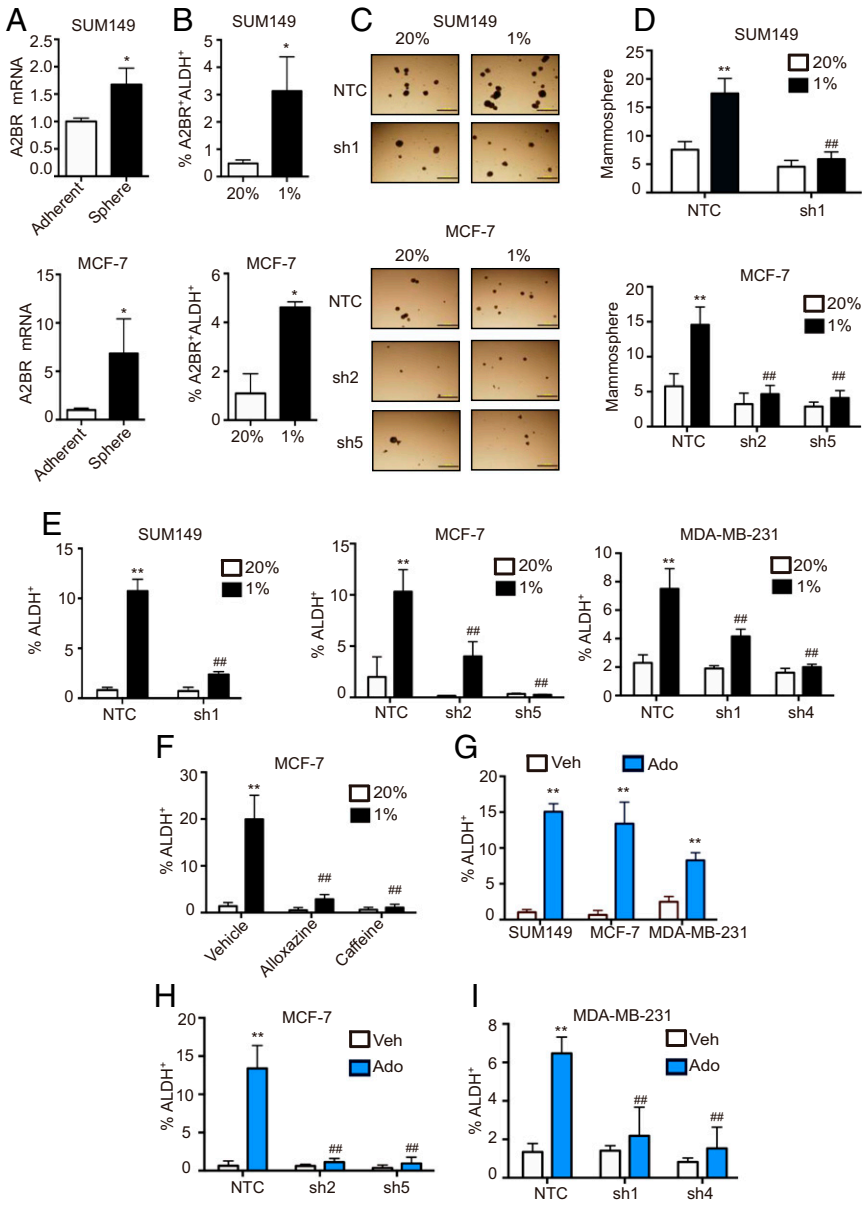

Fig. 2. A2BR expression enhances BCSC enrichment. (*A*) SUM149 (*Upper*) and MCF-7 (*Lower*) cells were cultured on standard polystyrene tissue culture plates (Adherent) or ultra-low attachment plates (Sphere) for 7 d and harvested for analysis of A2BR mRNA expression. Results were normalized to Adherent (mean ± SD; $n = 3$). $^{*}P < 0.05$ versus Adherent (Student's *t* test). (*B*) SUM149 (*Upper*) and MCF-7 (*Lower*) cells were exposed to 20% or 1% O_2 for 72 h, and the percentage of $A2BR^+ALDH^+$ cells was determined by flow cytometry (mean ± SD; $n = 3$). $^{*}P < 0.05$ versus 20% O_2 (Student's *t* test). (*C* and *D*) SUM149 (*Upper*) and MCF-7 (*Lower*) subclones transduced with lentiviral vector encoding NTC or an A2BR shRNA (sh1, sh2, or sh5) were exposed to 20% or 1% O_2 for 3 d, and then cells were cultured on ultra-low attachment plates for 7 d, and the number of mammospheres per field was counted (mean ± SD; $n = 3$). $^{**}P < 0.01$ versus NTC at 20% O_2; $^{\#\#}P < 0.01$ versus NTC at 1% O_2 (two-way ANOVA). (Scale bar: 1 mm.) (*E*) SUM149 (*Left*), MCF-7 (*Middle*), and MDA-MB-231 (*Right*) subclones transduced with NTC or an A2BR shRNA vector were exposed to 20% or 1% O_2 for 3 d, and the percentage of $ALDH^+$ cells was determined (mean ± SD; $n = 3$). $^{**}P < 0.01$ versus NTC at 20% O_2; $^{\#\#}P < 0.01$ versus NTC at 1% O_2 (two-way ANOVA). (*F*) MCF-7 cells were treated with vehicle, alloxazine (30 μM), or caffeine (8 μM) for 3 d, and the percentage of $ALDH^+$ cells was determined (mean ± SD; $n = 3$). $^{**}P < 0.01$ versus vehicle at 20% O_2; $^{\#\#}P < 0.01$ versus vehicle at 1% O_2 (two-way ANOVA). (*G*) Cells were treated with vehicle (Veh) or adenosine (Ado) for 3 d, and the percentage of $ALDH^+$ cells was determined (mean ± SD; $n = 3$). $^{**}P < 0.01$ versus Veh (two-way ANOVA). (*H* and *I*) MCF-7 (*H*) and MDA-MB-231 (*I*) subclones transfected with NTC or A2BR shRNA vector were treated with Ado (MCF-7, 5 μM; MDA-MB-231, 2.5 μM) for 3 d, and the percentage of $ALDH^+$ cells was determined (mean ± SD; $n = 3$). $^{**}P < 0.01$ versus NTC with Veh, $^{\#\#}P < 0.01$ versus NTC with Ado (two-way ANOVA).

stimulation in NTC but not in A2BR-knockdown (sh1 and sh4) subclones of MDA-MB-231 (*SI Appendix*, Fig. S6*C*). Taken together, these data suggest that PKCδ kinase activity is required for adenosine-induced and A2BR-mediated BCSC enrichment.

PKCδ has been reported to increase the phosphorylation of STAT3 at Ser-727 (S727) and thereby facilitate STAT3 nuclear translocation (42). Coadministration of a STAT3 inhibitor (i-STAT3) prevented the adenosine-induced increase in ALDH expression in MCF-7 (Fig. 4*E*) and MDA-MB-231 (*SI Appendix*, Fig. S6*B*) cells. RT-qRCR analysis revealed that the expression of mRNAs encoding NANOG and IL-6, two downstream targets of STAT3 that are required for the specification and/or maintenance of BCSCs (7), was increased by adenosine treatment of MCF-7 cells (Fig. 4*F*). IL-6 neutralizing antibody (IL-6 NAb) blocked the enrichment of $ALDH^+$ BCSCs in adenosine-treated MCF-7 (Fig. 4*G*) and MDA-MB-231 (*SI Appendix*, Fig. S6*B*) cells.

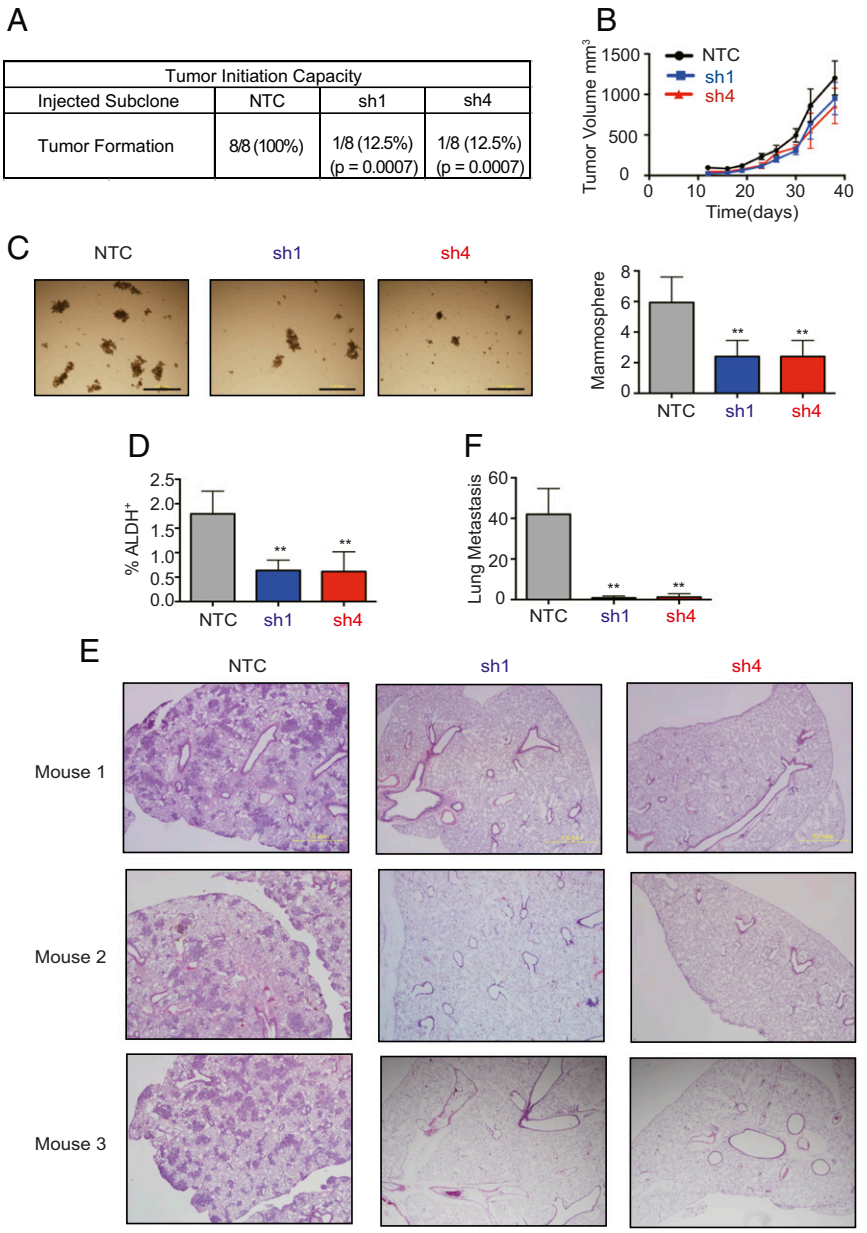

Fig. 3. Knockdown of A2BR inhibits tumor formation and metastasis. (*A*) MDA-MB-231 subclones (1×10^3 cells) transduced with NTC or an A2BR shRNA vector were implanted into the mammary fat pad (MFP). The proportion of mice with tumors after 11 wk and *P* value (vs. NTC; Fisher's exact test) are shown. (*B–F*) MDA-MB-231 subclones (2×10^6 cells) transduced with NTC or an A2BR shRNA vector were implanted into the MFP. Tumor volume (mean ± SD; $n = 6$–8 mice) was measured twice per week (*B*). When tumor volume reached 1,200 mm^3, primary tumors were harvested for mammosphere (*C*) and ALDH (*D*) assays (mean ± SD; $n = 3$). (Scale bar: 1 mm.) The number of mammospheres per field was counted (mean ± SD; $n = 15$); $^{**}P < 0.01$ versus NTC (one-way ANOVA). Lungs were harvested and fixed under inflation, paraffin-embedded sections were stained with hematoxylin and eosin (*E*) (scale bar: 1 mm), and the number of metastases per field was counted (*F*; mean ± SD; $n = 9$); $^{**}P < 0.01$ versus NTC (one-way ANOVA).

Next, we treated A2BR-knockdown and NTC subclones of MCF-7 and MDA-MB-231 with adenosine and performed immunoblot assays. Adenosine treatment increased the phosphorylation of specific Ser or Tyr residues of PKCδ (S645), STAT3 (S727 and Y705), and JAK2 (Y1007), and increased IL-6 and NANOG protein levels, in NTC subclones, and all of these effects were blocked by A2BR knockdown in MCF-7 (Fig. 4*H*) or MDA-MB-231 (*SI Appendix*, Fig. S6*C*) cells.

To determine the epistatic relationship between PKCδ, STAT3, and IL-6, we treated MCF-7 cells with i-PKCδ, pan-PKC inhibitor Ro31-8220, i-STAT3, or IL-6 NAb, and found that adenosine-induced phosphorylation of STAT3 was blocked by i-PKCδ (Fig. 4*I*) or Ro31-8220 (Fig. 4*J*). In contrast, adenosine-induced phosphorylation of PKCδ was not blocked by treatment with i-STAT3 (Fig. 4*K*) or IL-6 NAb (Fig. 4*L*). These results indicate that activation of A2BR leads to increased phosphorylation (at S645) and activation of PKCδ, which phosphorylates STAT3 (at S727), leading to transcriptional activation of the *NANOG* and *IL6* genes. IL-6, by binding to its cognate receptor, activates JAK2, a tyrosine kinase that phosphorylates STAT3 (at Y705), which is required for STAT3 nuclear translocation, completing a feedforward loop that amplifies A2BR-mediated signaling (Fig. 4*M*).

To further investigate whether hypoxia, which induces A2BR expression, activates the same signaling pathway induced by adenosine treatment, MCF-7 cells were treated with Ro31-8220,

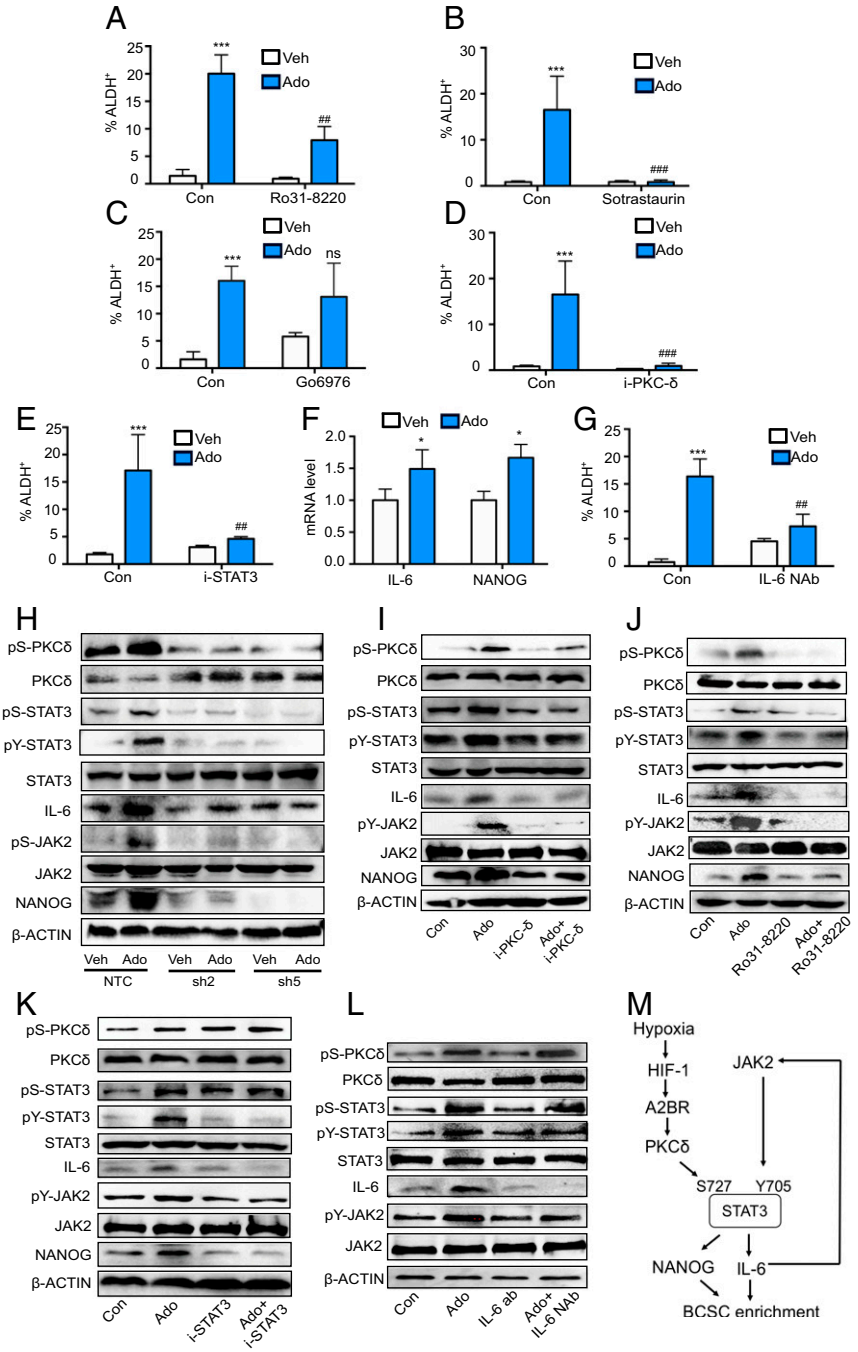

Fig. 4. A2BR promotes BCSC enrichment through PKCδ-dependent STAT3 activation. (*A–E*) MCF-7 cells were treated with vehicle (Veh) or 5 μM adenosine (Ado) in the absence (Con) or presence of a pan-PKC inhibitor [100 nM Ro31-8220 (*A*) or 1 nM sotrastaurin (*B*)], Ca^{2+}-dependent PKC subtype inhibitor [15 μM Go6976 (*C*)], PKCδ inhibitor [100 nM i-PKCδ (*D*)], or STAT3 inhibitor VII [100 nM i-STAT3 (*E*)] for 3 d, and the percentage of $ALDH^+$ cells was determined (mean ± SD; $n = 3$). $^{***}P < 0.001$ versus control (Con) treated with vehicle (Veh); $^{\#\#}P < 0.01$, $^{\#\#\#}P < 0.001$, and ns (no significant difference) versus Con treated with Ado (two-way ANOVA). (*F*) MCF-7 cells were treated with Veh or Ado for 3 d, and IL-6 and NANOG mRNA levels were determined by RT-qPCR (mean ± SD; $n = 3$); $^{*}P < 0.05$ versus Veh. (*G*) MCF-7 cells were treated with Veh or Ado for 3 d in the absence or presence of IL-6 neutralizing antibody (2.5 μg/mL IL-6 NAb), and the percentage of $ALDH^+$ cells was determined (mean ± SD; $n = 3$). $^{***}P < 0.001$ versus control (Con) treated with vehicle (Veh); $^{\#\#}P < 0.01$ versus Con treated with Ado (two-way ANOVA). (*H*) MCF-7 subclones transduced with NTC or an A2BR shRNA (sh2 or sh5) vector were treated with Veh (Con) or Ado for 3 d, and immunoblot assays were performed. (*I–L*) MCF-7 cells were treated with vehicle (Con) or Ado, either alone or in combination with i-PKCδ (*I*), Ro31-8220 (*J*), i-STAT3 (*K*), or IL-6 NAb (*L*) for 3 d, and immunoblot assays were performed. (*M*) Hypoxia induces A2BR expression in a HIF-1α–dependent manner and increases A2BR–PKCδ–STAT3 signaling, resulting in augmented expression of IL-6 and NANOG, which specify the BCSC phenotype.

i-PKCδ, i-STAT3, or IL-6 NAb for 72 h at 20% or 1% O_2. Each of these inhibitors blocked hypoxia-induced enrichment of $ALDH^+$ BCSCs (Fig. 5*A*). We also exposed MCF-7 NTC and A2BR-knockdown subclones to 20% or 1% O_2 for 48 h, and found that hypoxia increased the phosphorylation of PKCδ, STAT3, and JAK2, and the expression of IL-6 and NANOG, all of which were blocked by A2BR knockdown in the sh2 and sh5 subclones of MCF-7 (Fig. 5*B*). These results indicate that the

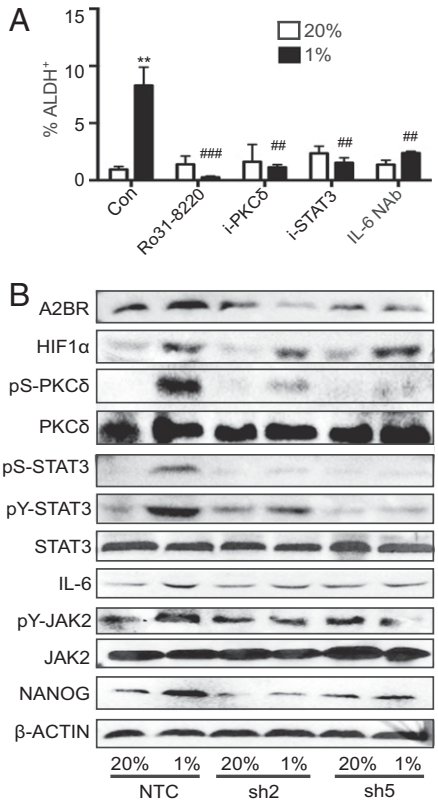

Fig. 5. Hypoxia induces BCSC enrichment through A2BR–PKCδ–STAT3 signaling. (*A*) MCF-7 cells were treated with vehicle (Con), 100 nM Ro31-8220, 100 nM i-PKCδ, 100 nM i-STAT3, or 2.5 μg/mL IL-6 NAb, and exposed to 20% or 1% O_2 for 3 d. The percentage of $ALDH^+$ cells (mean ± SD; $n = 3$) was determined by flow cytometry. $^{**}P < 0.001$ versus Con cells at 20% O_2; $^{\#\#}P < 0.01$, $^{\#\#\#}P < 0.001$ versus Con cells at 1% O_2 (two-way ANOVA). (*B*) MCF-7 subclones stably transduced with NTC or A2BR shRNA vector were exposed to 20% or 1% O_2 for 48 h, and immunoblot assays were performed.

A2BR–PKCδ–STAT3 signaling pathway (amplified by JAK2–STAT3–IL-6 signaling) is required for hypoxia-induced BCSC enrichment.

To investigate whether A2BR activates the PKCδ–STAT3 pathway in vivo, we performed orthotopic implantation of MDA-MB-231 NTC or A2BR knockdown cells into the MFP of female SCID mice and harvested tumors when they reached a volume of 1,200 mm^3. Immunoblot assays revealed that phosphorylation of PKCδ (S645), STAT3 (S727 and Y705), and JAK2 (Y1007), as well as expression of IL-6 and NANOG, were decreased in A2BR-knockdown tumors compared with NTC tumors (Fig. 6). These results indicate that the same signaling pathways that were activated in vitro by exposure of breast cancer cells to hypoxia or adenosine, were activated in the tumor microenvironment in vivo.

Discussion

Hypoxia, which is a critical factor for cancer progression (7), has been reported to increase adenosine production through increased expression of CD39 and CD73 and/or decreased expression of adenosine kinase (14, 31, 43). In the present study, we found that hypoxia also increases expression of adenosine receptor A2BR in human breast cancer cells in a HIF-1α–dependent manner. A2BR stimulates PKCδ–STAT3 signaling, which is required for hypoxia-induced BCSC enrichment. Our findings suggest that therapeutic targeting of A2BR might increase the probability of eradicating BCSCs in patients with breast cancer.

Recently, A2BR has been associated with cancer progression. A2BR expression is increased in both colorectal and prostate cancer cell lines, and A2BR inhibition decreased cancer cell proliferation (25, 26, 44). In lung cancer cells, A2BR modulates the epithelial–mesenchymal transition by shifting the balance between the PKA and ERK pathways (45). In breast cancer cell lines, activation of A2BR suppresses prenylation of the small guanosine triphosphatase Rap1B—thereby promoting cell scattering (46)—and stimulates metastasis (27–30). Overexpression of A2BR in the nontumorigenic NMuMG mouse mammary cell line enabled tumor formation (47). In the present study, we demonstrate a role of A2BR in BCSC enrichment. Genetic or pharmacological inhibition of A2BR expression or activity, respectively, abrogated BCSC enrichment in response to adenosine or hypoxia, and decreased tumorigenic capacity and lung metastasis in vivo by decreasing the BCSC population. Since BCSCs are required for breast cancer recurrence and metastasis (6), which are the major causes of breast cancer-related mortality, therapeutic targeting of A2BR may increase patient survival.

Adenosine is an extracellular signaling molecule, the concentration of which is markedly increased in many tumors (48). Upon binding to its cognate receptors, adenosine can activate several different downstream signaling pathways. The classical signaling pathway downstream of A2BR, which recruits Gs/Gq proteins, serves to increase the activity of adenylyl cyclase, leading to the serial activation of PKA, PLC, and PKC (49, 50). However, rather than conventional Ca^{2+}-activated PKCs, we demonstrated that PKCδ, a Ca^{2+}-independent isoform, is involved in the regulation of BCSCs downstream of A2BR by phosphorylation of STAT3 on Ser-727, which increases its transcriptional activity. PKCδ inhibitors (such as KAI-9803, delcasertib, and rottlerin) have already passed phase I clinical trials for cardiovascular diseases (51, 52). Trials designed to test whether those drugs are safe and effective in breast cancer patients should be considered based on the data presented above.

In addition to the PKCδ–STAT3 signaling pathway, A2BR may regulate the BCSC phenotype through other mechanisms. In MDA-MB-231 cells, it has been reported that A2BR inhibits ERK1/2 phosphorylation (28). Loss of ERK1/2 activity may cause transcriptional activation of *NANOG* through dephosphorylation and nuclear translocation of FOXO3 (53). In endothelial cells, A2BR signaling stimulates the release of IL-8, FGF-2, and VEGF-A, each of which may contribute to BCSC

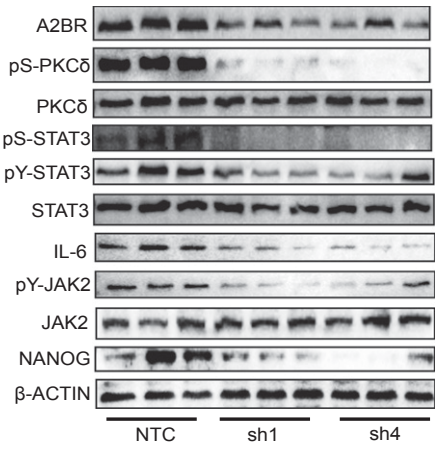

Fig. 6. NANOG expression in orthotopic breast tumors is dependent upon A2BR–PKCδ–STAT3 signaling. MDA-MB-231 subclones (2×10^6 cells) transduced with NTC or either of two A2BR shRNA vectors (sh1 or sh4) were implanted into the MFP. When tumor volume reached 1,200 mm^3, tumors were harvested for immunoblot assays.

enrichment (54). Thus, further analysis of signaling pathways downstream of A2BR is needed to fully understand the role of A2BR in BCSC enrichment.

Accumulation of extracellular adenosine in the tumor microenvironment suppresses antitumor immunity mediated by natural killer cells and $CD8^+$ T cells through A2AR signaling, and antitumor immunity can be restored by genetic or pharmacological inhibition of A2AR on immune cells (14, 55, 56). Extensive preclinical data indicate that A2AR inhibition increases antitumor immunity mediated by T cells and slows tumor growth (57–59), which has led to the development of A2AR antagonists as anticancer therapeutics. Here, we report that genetic or pharmacological inhibition of A2BR decreased the BCSC population in orthotopic tumors. Thus, targeting both A2AR and A2BR may further increase tumor control by activation of the immune system and inhibition of the BCSC phenotype.

Hypoxia plays an important role in tumor progression. We previously reported that hypoxia increases adenosine production by breast cancer cells in a HIF-1α–dependent manner (31). The coexpression of both CD73, which generates adenosine, and A2BR, which is activated in response to adenosine binding, constitutes an autocrine signaling pathway leading to STAT3-dependent expression of NANOG, a pluripotency factor that specifies the BCSC phenotype. These findings may explain previous studies reporting that CD73 activity promoted the BCSC phenotype (60). We previously reported that hypoxia induces HIF-dependent demethylation of N^6-methyladenosine residues leading to stabilization of NANOG mRNA, thereby stimulating BCSC accumulation (61, 62). Thus, HIF-1 induces NANOG expression by both transcriptional and posttranscriptional mechanisms in hypoxic breast cancer cells. Hypoxia also induces HIF-dependent expression of CD47, which, as with CD73, plays dual roles in promoting BCSC and immune evasion phenotypes (31, 63). Taken together, these studies suggest that therapeutic targeting of HIF-1 may increase the probability of BCSC eradication and thereby increase the survival of breast cancer patients.

Materials and Methods

Cell Lines and Tissue Culture. MCF-7 and MDA-MB-231 cells were maintained in high-glucose (4.5 mg/mL) DMEM. SUM149 and SUM159 cells were maintained in DMEM/F12 (50:50) medium. All culture media were supplemented with 10% (vol/vol) FBS and 1% (vol/vol) penicillin–streptomycin. All cells were maintained at 37 °C in a 5% CO_2, 95% air incubator (20% O_2). Hypoxic cells were maintained at 37 °C in a modular incubator chamber (Billups–Rothenberg) flushed with a gas mixture containing 1% O_2, 5% CO_2, and 94% N_2. All chemicals are listed in *SI Appendix*, Table S1.

Lentivirus Transduction. Lentiviral vectors encoding shRNA targeting HIF-1α or HIF-2α, as well as the NTC shRNA, were described previously (34, 64). Lentiviral vectors encoding shRNA targeting A2BR mRNA were purchased from Sigma-Aldrich (clone numbers are listed in *SI Appendix*, Table S2). All lentiviral shuttle vectors were transfected into 293T cells for packaging. Viral supernatant was collected after 48 h and used for transduction of human breast cancer cell lines as described previously (64). Puromycin (0.5 μg/mL) was added to the medium of cells transduced with lentivirus for selection of pools of cells expressing the shRNA.

RT-qPCR. RNA was extracted using TRIzol (Invitrogen) and cDNA synthesis was performed according to the manufacturer's instructions (Applied Biosystems). qPCR was performed using SYBR Green qPCR Master Mix (Bio-Rad). The expression of each target mRNA relative to 18S rRNA was calculated based on the threshold cycle (Ct) as $2^{-\Delta(\Delta Ct)}$, where $\Delta Ct = Ct_{target} - Ct_{18S}$ and $\Delta(\Delta Ct) = \Delta Ct_{treatment} - \Delta Ct_{control}$. Nucleotide sequences of primers are shown in *SI Appendix*, Table S3.

Immunoblot Assay. Whole-cell lysates were prepared in modified RIPA lysis buffer (50 mM Tris·HCl, pH 7.5, 1 mM β-mercaptoethanol, 150 mM NaCl, 1 mM Na_3VO_4, 1 mM NaF, 1 mM EDTA, 0.25% sodium deoxycholate, and 1% Igepal CA-630). Blots were probed with antibodies against HIF-1α, A2BR, p-PKCδ(S645), PKCδ, p-STAT3(S727), p-STAT3(Y705), STAT3, IL-6, p-JAK2 (Y1007), JAK2, NANOG, or β-Actin (see *SI Appendix*, Table S4 for vendors). HRP-conjugated anti-rabbit and anti-mouse secondary antibodies were used, and the chemiluminescent signal was detected using ECL Plus (GE Healthcare).

Flow Cytometry. Cultured cells were trypsinized and incubated with Fc Block (BD Pharmingen). $A2BR^+$ cells were identified by staining with phycoerythrin-conjugated anti-A2BR antibody (Novus Biologicals). Samples were analyzed by flow cytometry (FACSCalibur; BD Biosciences). Unstained control and single-stained cells were prepared in every experiment for gating. Dead cells were gated out by side-scatter and forward-scatter analysis.

ALDH Assay. Cultured cells were trypsinized, whereas tumor tissues were minced, digested with type 1 collagenase (1 mg/mL; Sigma-Aldrich) at 37 °C for 30 min, and filtered through a 70-mm cell strainer. A total of 1×10^6 cells was suspended in buffer containing 1 mM BODIPY-aminoacetaldehyde (STEMCELL Technologies), incubated at 37 °C for 45 min, and analyzed by flow cytometry. An aliquot from each sample was treated with 50 mM diethylaminobenzaldehyde, an ALDH inhibitor, as a negative control for gating.

Mammosphere Assay. Cultured cells were trypsinized, whereas tumor tissues were minced and digested with 1 mg/mL type 1 collagenase (Sigma-Aldrich) at 37 °C for 30 min to prepare single-cell suspensions, which were seeded in six-well ultra-low attachment plates (Corning) at a density of 5,000 cells per mL in Complete MammoCult Medium (STEMCELL Technologies). After 7 d, the cells were photographed under an Olympus TH4-100 microscope, and the number of mammospheres with a diameter ≥70 μm was counted using ImageJ software (NIH).

ChIP. MCF-7 cells were incubated at 20% or 1% O_2 for 16 h, cross-linked in 3.7% formaldehyde for 15 min, quenched in 0.125 M glycine for 5 min, and lysed with SDS lysis buffer. Chromatin was sheared by sonication, and lysates were precleared with salmon sperm DNA/protein A agarose slurry (Millipore) for 1 h and incubated with IgG or antibody against HIF-1α, HIF-1β, or HIF-2α (*SI Appendix*, Table S4) in the presence of protein A–agarose beads overnight. After serial washing of the agarose beads with low-salt, high-salt, and LiCl buffers, DNA was eluted in 1% SDS with 0.1 M $NaHCO_3$, and cross-links were reversed by addition of 0.2 M NaCl. DNA was purified by phenol–chloroform extraction and ethanol precipitation, and analyzed by qPCR (see *SI Appendix*, Table S5 for primer sequences).

Mouse Studies. Protocols were approved by the Johns Hopkins University Animal Care and Use Committee and were in accordance with the NIH *Guide for the Care and Use of Laboratory Animals* (65). For the tumor initiation study, 1×10^3 breast cancer cells were injected into the MFP of 6- to 8-wk-old female SCID mice in a 1:1 suspension of Matrigel (BD Biosciences) in PBS. For other experiments, 2×10^6 cells were injected.

Statistical Analysis. Data are expressed as mean ± SD. The Pearson correlation coefficient (R) was used to compare the expression of mRNA encoding adenosine receptors with the HIF signature, which was based on mRNA data from TCGA Breast Invasive Carcinoma dataset of 1,095 patients (66). For the tumor initiation assay, Fisher's exact test was performed. For all other assays, differences between two groups were analyzed by Student's t test, whereas differences between multiple groups were analyzed by ANOVA. Values of $P < 0.05$ were considered significant for all analyses.

ACKNOWLEDGMENTS. We thank Karen Padgett of Novus Biologicals for providing IgG and antibodies against A2BR, HIF-1β, HIF-2α, p-PKCδ (S645), PKCδ, p-STAT3 (S727), p-STAT3 (Y705), p-JAK2 (Y1007), JAK2, and NANOG. G.L.S. is an American Cancer Society Research Professor and the C. Michael Armstrong Professor at the Johns Hopkins University School of Medicine. This work was supported by the Emerson Collective Cancer Research Fund, American Cancer Society, and the Cindy Rosencrans Fund for Triple-Negative Breast Cancer.

1. Siegel RL, Miller KD, Jemal A (2017) Cancer statistics, 2017. *CA Cancer J Clin* 67:7–30.
2. Al-Hajj M, Wicha MS, Benito-Hernandez A, Morrison SJ, Clarke MF (2003) Prospective identification of tumorigenic breast cancer cells. *Proc Natl Acad Sci USA* 100:3983–3988.
3. Ponti D, et al. (2005) Isolation and in vitro propagation of tumorigenic breast cancer cells with stem/progenitor cell properties. *Cancer Res* 65:5506–5511.
4. Bozorgi A, Khazaei M, Khazaei MR (2015) New findings on breast cancer stem cells: A review. *J Breast Cancer* 18:303–312.
5. Al-Ejeh F, et al. (2011) Breast cancer stem cells: Treatment resistance and therapeutic opportunities. *Carcinogenesis* 32:650–658.
6. Oskarsson T, Batlle E, Massagué J (2014) Metastatic stem cells: Sources, niches, and vital pathways. *Cell Stem Cell* 14:306–321.

7. Semenza GL (2016) The hypoxic tumor microenvironment: A driving force for breast cancer progression. *Biochim Biophys Acta* 1863:382–391.
8. Rankin EB, Nam JM, Giaccia AJ (2016) Hypoxia: Signaling the metastatic cascade. *Trends Cancer* 2:295–304.
9. Wilson WR, Hay MP (2011) Targeting hypoxia in cancer therapy. *Nat Rev Cancer* 11: 393–410.
10. Conley SJ, et al. (2012) Antiangiogenic agents increase breast cancer stem cells via the generation of tumor hypoxia. *Proc Natl Acad Sci USA* 109:2784–2789.
11. Taylor CT, Colgan SP (2017) Regulation of immunity and inflammation by hypoxia in immunological niches. *Nat Rev Immunol* 17:774–785.
12. Semenza GL (2012) Hypoxia-inducible factors in physiology and medicine. *Cell* 148: 399–408.
13. Yegutkin GG (2014) Enzymes involved in metabolism of extracellular nucleotides and nucleosides: Functional implications and measurement of activities. *Crit Rev Biochem Mol Biol* 49:473–497.
14. Sitkovsky M, Ohta A (2013) Targeting the hypoxia-adenosinergic signaling pathway to improve the adoptive immunotherapy of cancer. *J Mol Med (Berl)* 91:147–155.
15. Layland J, Carrick D, Lee M, Oldroyd K, Berry C (2014) Adenosine: Physiology, pharmacology, and clinical applications. *JACC Cardiovasc Interv* 7:581–591.
16. Fredholm BB (2007) Adenosine, an endogenous distress signal, modulates tissue damage and repair. *Cell Death Differ* 14:1315–1323.
17. Fredholm BB, et al. (1994) Nomenclature and classification of purinoceptors. *Pharmacol Rev* 46:143–156.
18. Borea PA, Gessi S, Merighi S, Varani K (2016) Adenosine as a multi-signalling guardian angel in human diseases: When, where and how does it exert its protective effects? *Trends Pharmacol Sci* 37:419–434.
19. Sitaraman SV, et al. (2001) Neutrophil-epithelial crosstalk at the intestinal lumenal surface mediated by reciprocal secretion of adenosine and IL-6. *J Clin Invest* 107: 861–869.
20. Lynge J, Schulte G, Nordsborg N, Fredholm BB, Hellsten Y (2003) Adenosine A 2B receptors modulate cAMP levels and induce CREB but not ERK1/2 and p38 phosphorylation in rat skeletal muscle cells. *Biochem Biophys Res Commun* 307: 180–187.
21. Schulte G, Fredholm BB (2003) Signalling from adenosine receptors to mitogen-activated protein kinases. *Cell Signal* 15:813–827.
22. Kong T, Westerman KA, Faigle M, Eltzschig HK, Colgan SP (2006) HIF-dependent induction of adenosine A2B receptor in hypoxia. *FASEB J* 20:2242–2250.
23. Poth JM, Brodsky K, Ehrentraut H, Grenz A, Eltzschig HK (2013) Transcriptional control of adenosine signaling by hypoxia-inducible transcription factors during ischemic or inflammatory disease. *J Mol Med (Berl)* 91:183–193.
24. Ryzhov S, et al. (2011) Adenosinergic regulation of the expansion and immunosuppressive activity of $CD11b^{+}Gr1^{+}$ cells. *J Immunol* 187:6120–6129.
25. Wei Q, Costanzi S, Balasubramanian R, Gao ZG, Jacobson KA (2013) A2B adenosine receptor blockade inhibits growth of prostate cancer cells. *Purinergic Signal* 9: 271–280.
26. Vecchio EA, et al. (2016) Ligand-independent adenosine A2B receptor constitutive activity as a promoter of prostate cancer cell proliferation. *J Pharmacol Exp Ther* 357: 36–44.
27. Desmet CJ, et al. (2013) Identification of a pharmacologically tractable Fra-1/ADORA2B axis promoting breast cancer metastasis. *Proc Natl Acad Sci USA* 110: 5139–5144.
28. Mittal D, et al. (2016) Adenosine 2B receptor expression on cancer cells promotes metastasis. *Cancer Res* 76:4372–4382.
29. Cekic C, et al. (2012) Adenosine A2B receptor blockade slows growth of bladder and breast tumors. *J Immunol* 188:198–205.
30. Stagg J, et al. (2010) Anti-CD73 antibody therapy inhibits breast tumor growth and metastasis. *Proc Natl Acad Sci USA* 107:1547–1552.
31. Samanta D, et al. (2018) Chemotherapy induces enrichment of $CD47^{+}/CD73^{+}/PDL1^{+}$ immune evasive triple-negative breast cancer cells. *Proc Natl Acad Sci USA* 115: E1239–E1248.
32. Parker JS, et al. (2009) Supervised risk predictor of breast cancer based on intrinsic subtypes. *J Clin Oncol* 27:1160–1167.
33. Samanta D, Gilkes DM, Chaturvedi P, Xiang L, Semenza GL (2014) Hypoxia-inducible factors are required for chemotherapy resistance of breast cancer stem cells. *Proc Natl Acad Sci USA* 111:E5429–E5438.
34. Xiang L, et al. (2014) Hypoxia-inducible factor 1 mediates TAZ expression and nuclear localization to induce the breast cancer stem cell phenotype. *Oncotarget* 5: 12509–12527.
35. Zhang H, et al. (2008) Digoxin and other cardiac glycosides inhibit HIF-1alpha synthesis and block tumor growth. *Proc Natl Acad Sci USA* 105:19579–19586.
36. Lee K, et al. (2009) Acriflavine inhibits HIF-1 dimerization, tumor growth, and vascularization. *Proc Natl Acad Sci USA* 106:17910–17915.
37. Semenza GL, et al. (1996) Hypoxia response elements in the aldolase A, enolase 1, and lactate dehydrogenase A gene promoters contain essential binding sites for hypoxia-inducible factor 1. *J Biol Chem* 271:32529–32537.
38. Dontu G, et al. (2003) In vitro propagation and transcriptional profiling of human mammary stem/progenitor cells. *Genes Dev* 17:1253–1270.
39. Ginestier C, et al. (2007) ALDH1 is a marker of normal and malignant human mammary stem cells and a predictor of poor clinical outcome. *Cell Stem Cell* 1:555–567.
40. Yang Y, et al. (2015) Involvement of cAMP-PKA pathway in adenosine A1 and A2A receptor-mediated regulation of acetaldehyde-induced activation of HSCs. *Biochimie* 115:59–70.
41. Chen Y, et al. (2017) Endogenous Gαq-coupled neuromodulator receptors activate protein kinase A. *Neuron* 96:1070–1083.e5.
42. Gartsbein M, et al. (2006) The role of protein kinase C delta activation and STAT3 Ser727 phosphorylation in insulin-induced keratinocyte proliferation. *J Cell Sci* 119: 470–481.
43. Ohta A (2016) A metabolic immune checkpoint: Adenosine in tumor microenvironment. *Front Immunol* 7:109.
44. Ma DF, et al. (2010) Hypoxia-inducible adenosine A2B receptor modulates proliferation of colon carcinoma cells. *Hum Pathol* 41:1550–1557.
45. Giacomelli C, et al. (2018) The A_{2B} adenosine receptor modulates the epithelial-mesenchymal transition through the balance of cAMP/PKA and MAPK/ERK pathway activation in human epithelial lung cells. *Front Pharmacol* 9:54.
46. Ntantie E, et al. (2013) An adenosine-mediated signaling pathway suppresses prenylation of the GTPase Rap1B and promotes cell scattering. *Sci Signal* 6:ra39.
47. Ihara T, et al. (2017) An in vivo screening system to identify tumorigenic genes. *Oncogene* 36:2023–2029.
48. Gessi S, Merighi S, Varani K, Borea PA (2011) Adenosine receptors in health and disease. *Adv Pharmacol* 61:41–75.
49. Ryzhov S, Goldstein AE, Biaggioni I, Feoktistov I (2006) Cross-talk between G_s- and G_q-coupled pathways in regulation of interleukin-4 by A_{2B} adenosine receptors in human mast cells. *Mol Pharmacol* 70:727–735.
50. Ryzhov S, et al. (2009) Differential role of the carboxy-terminus of the A_{2B} adenosine receptor in stimulation of adenylate cyclase, phospholipase Cbeta, and interleukin-8. *Purinergic Signal* 5:289–298.
51. Lincoff AM, et al.; PROTECTION AMI Investigators (2014) Inhibition of delta-protein kinase C by delcasertib as an adjunct to primary percutaneous coronary intervention for acute anterior ST-segment elevation myocardial infarction: Results of the PROTECTION AMI randomized controlled trial. *Eur Heart J* 35:2516–2523.
52. Bates E, et al.; Direct Inhibition of delta-Protein Kinase C Enzyme to Limit Total Infarct Size in Acute Myocardial Infarction (DELTA MI) Investigators (2008) Intracoronary KAI-9803 as an adjunct to primary percutaneous coronary intervention for acute ST-segment elevation myocardial infarction. *Circulation* 117:886–896.
53. Lu H, et al. (2015) Chemotherapy triggers HIF-1-dependent glutathione synthesis and copper chelation that induces the breast cancer stem cell phenotype. *Proc Natl Acad Sci USA* 112:E4600–E4609.
54. Feoktistov I, et al. (2002) Differential expression of adenosine receptors in human endothelial cells: Role of A2B receptors in angiogenic factor regulation. *Circ Res* 90: 531–538.
55. Häusler SF, et al. (2011) Ectonucleotidases CD39 and CD73 on OvCA cells are potent adenosine-generating enzymes responsible for adenosine receptor 2A-dependent suppression of T cell function and NK cell cytotoxicity. *Cancer Immunol Immunother* 60: 1405–1418.
56. Ohta A, et al. (2006) A2A adenosine receptor protects tumors from antitumor T cells. *Proc Natl Acad Sci USA* 103:13132–13137.
57. Eini H, et al. (2015) Caffeine promotes anti-tumor immune response during tumor initiation: Involvement of the adenosine A2A receptor. *Biochem Pharmacol* 98: 110–118.
58. Ma SR, et al. (2017) Blockade of adenosine A2A receptor enhances $CD8^{+}$ T cells response and decreases regulatory T cells in head and neck squamous cell carcinoma. *Mol Cancer* 16:99.
59. Mediavilla-Varela M, et al. (2017) A novel antagonist of the immune checkpoint protein adenosine A2A receptor restores tumor-infiltrating lymphocyte activity in the context of the tumor microenvironment. *Neoplasia* 19:530–536.
60. Yu J, et al. (2017) A preliminary study of the role of extracellular -5′- nucleotidase in breast cancer stem cells and epithelial-mesenchymal transition. *In Vitro Cell Dev Biol Anim* 53:132–140.
61. Zhang C, et al. (2016) Hypoxia induces the breast cancer stem cell phenotype by HIF-dependent and ALKBH5-mediated m^6A-demethylation of NANOG mRNA. *Proc Natl Acad Sci USA* 113:E2047–E2056.
62. Zhang C, et al. (2016) Hypoxia-inducible factors regulate pluripotency factor expression by ZNF217- and ALKBH5-mediated modulation of RNA methylation in breast cancer cells. *Oncotarget* 7:64527–64542.
63. Zhang H, et al. (2015) HIF-1 regulates CD47 expression in breast cancer cells to promote evasion of phagocytosis and maintenance of cancer stem cells. *Proc Natl Acad Sci USA* 112:E6215–E6223.
64. Zhang H, et al. (2012) HIF-1-dependent expression of angiopoietin-like 4 and L1CAM mediates vascular metastasis of hypoxic breast cancer cells to the lungs. *Oncogene* 31:1757–1770.
65. National Research Council (2011) *Guide for the Care and Use of Laboratory Animals* (National Academies Press, Washington, DC), 8th Ed.
66. Cancer Genome Atlas Network (2012) Comprehensive molecular portraits of human breast tumours. *Nature* 490:61–70.